Effect of Temperature and Chain Length on the Bimodal Emission Properties of Single Polyfluorene Copolymer Molecules†

John K. Grey,‡ Doo Young Kim,‡ Carrie L. Donley,§ William L. Miller,‡ Ji Seon Kim,§ Carlos Silva,|| Richard H. Friend,§ and Paul F. Barbara*,‡

Center for Nano and Molecular Science and Technology and Department of Chemistry and Biochemistry, University of Texas at Austin, Austin, Texas 78712, Cavendish Laboratory, University of Cambridge, Madingley Road, Cambridge CB3 0HE, United Kingdom, and Département de Physique, C.P. 6128 Université de Montreal, Montreal, Québec H3C 3J7, Canada

Received: December 16, 2005; In Final Form: March 6, 2006

Fluorescence emission spectra were recorded for isolated polymer chains of the polyfluorene copolymer, F8BT [poly(9,9-di-*n*-octylfluorene-*alt*-benzothiadiazole)], at 298 and 20 K for two molecular weights (chain lengths). For long-chain F8BT at 298 K, the observed *distribution of single-molecule* emission maxima $G(E_{max})$ is bimodal, with peaks at ∼2.35 eV ("blue") and ∼2.25 eV ("red"). Previously, the red forms have been assigned to polymer chains that possess intrachain contacts, which lowers the local singlet exciton energy. At ∼20 K, $G(E_{max})$ collapses into a single broad distribution centered at ∼2.3 eV for long-chain F8BT. However, this distribution can be further divided into a high-energy edge that is dominated by the "blue" form, while the remainder of the distribution is composed of the "red" form. Low-molecular-weight F8BT samples emit exclusively from the blue form, and no shift in peak maxima with low temperature was observed. A Franck−Condon analysis reveals a decrease in emitting state displacements between spectra measured at 298 and 20 K, suggesting that temperature-induced structural displacements are responsible for the change in the bimodal emission.

Introduction

A rigorous understanding of how the emission properties of conjugated polymer films depend on morphology is critical toward advancing the many promising applications of these materials. It is generally accepted that the bulk emission spectra of conjugated polymers are essentially a sum of individual spectral components, each associated with a different quasilocalized one-dimensional chromophore on the polymer chains. Various types of evidence suggest that the distribution of chromophore transition energies for conjugated polymers can be significantly broadened and red-shifted due to the presence of specific morphological features. These features have been alternatively attributed to chain−chain contacts,[1−3] polymer chain aggregation,[4−6] and conformational states of the polymer chain.[7−11]

Recently, single-molecule spectroscopy (SMS) on isolated conjugated polymer chains[2,3,11−17] and other multichromophoric systems[18−23] has provided new information on the distribution of chromophore transition energies. SM spectra are significantly less inhomogeneously broadened than bulk spectra, allowing for a more detailed analysis. In addition, observation of emission from high-energy "blue" chromophores is more common in isolated polymer chain vs bulk polymer samples due to the absence of *inter*molecular energy transfer to low-energy sites in the former case. For example, SMS studies on the prototypical polymer MEH-PPV have revealed distinct "blue" and "red", chromophores both corresponding to localized $\pi-\pi^*$ transitions

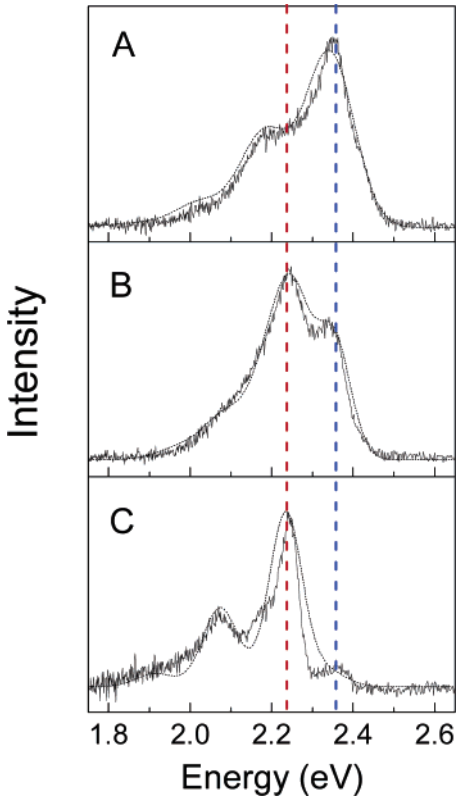

Figure 1. Typical single-molecule (SM) spectra of *long*-chain F8BT samples (solid lines) with fitted spectra (dashed lines) measured at 20 K. Spectra are classified according to peak wavelength maxima, revealing three forms: (A) "blue", (B) "mixed" (blue and red), and (C) "red". Dotted vertical lines running through the panels highlight the average peak maxima for the blue and red forms.

† Part of the special issue "Robert J. Silbey Festschrift".

* Corresponding author. E-mail: p.barbara@mail.utexas.edu.
‡ Center for Nano and Molecular Science and Technology and Department of Chemistry and Biochemistry, University of Texas at Austin.
§ Cavendish Laboratory, University of Cambridge.
|| Département de Physique, C.P. 6128 Université de Montreal.

10.1021/jp057361r CCC: $33.50
Published on Web 04/07/2006

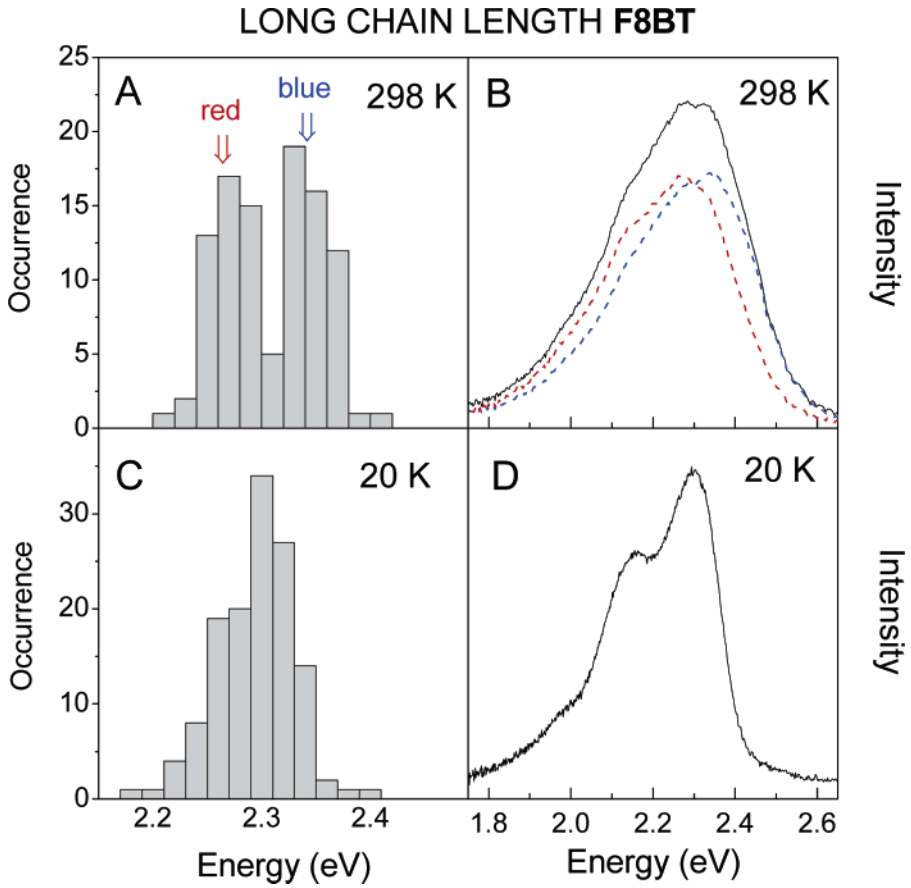

Figure 2. Emission peak energy distributions and ensemble emission spectra for isolated *long* chains of F8BT dissolved in a PMMA thin film at 298 K (A, B) and 20 K (C, D). The two components of the bimodal peak energy distribution in (A) have been labeled "blue" (high-energy component) and "red" (low-energy component). Sorted subensemble spectra are shown for the 298 K long-chain F8BT data (panel B) based on the "blue" and "red" peak energy maxima, E_{max}.

SCHEME 1: Chemical Structure of F8BT

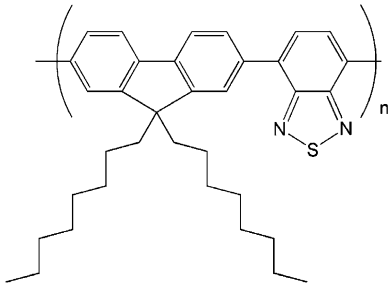

on the polymer chains.[2,15] The low-energy "red" states arise from molecular packing effects (chain−chain contacts), which are more prevalent in collapsed chain conformations.[2,3] Recent low-temperature and variable-molecular-weight (MW) SMS studies of MEH-PPV have shown that the number of red-emitting species increase as the molecular weight (chain length) is increased.[15] This effect is due to an increased probability for intramolecular chain−chain contacts as the polymer chain length increases, leading to efficient energy transfer to red sites.

In this paper, we apply a similar approach to investigate the effect of polymer chain length and temperature on the emission properties of the polyfluorene copolymer F8BT [poly(9,9-di-*n*-octylfluorene-*alt*-benzothiadiazole)] (Scheme 1). F8BT is a highly emissive polyfluorene derivative that has seen widespread use in light-emitting diode[24,25] and photovoltaic device applications as an electron acceptor material.[26−30] Recent room-temperature (298 K) SMS work on F8BT has also demonstrated that emission from low-energy (red) sites increases with chain length.[31] However, only broad and unresolved emission line shapes are observed at 298 K, making it difficult to definitively classify the types of emitting species present in single F8BT polymer chains. This problem can be overcome by using low-temperature SMS, which affords better spectral resolution and permits a detailed molecule-by-molecule analysis of energy migration in single polymer chains.

Experimental Section

F8BT samples of short chain (M_n = 9 kDa, polydispersity index = 3.45) and long chain (M_n = 90 kDa, polydispersity index = 1.99) were synthesized according to ref 32, where M_n is the number-averaged molecular weight. Dilute thin film samples were prepared by dissolving the samples into a suitable solvent (chloroform) and diluting into a toluene solution of PMMA (3% w/w). Solutions were spin-cast onto glass substrates and sealed with Au or Al to prevent oxygen from diffusing into the films. Images and spectra were acquired using a scanning confocal microscope with the sample temperature regulated by a "coldfinger" liquid helium cryostat, described in detail elsewhere.[15,33] Samples were excited with the 457.9-nm line of an argon−ion laser, and emitted light was filtered with holographic notch filters to remove scattered excitation and dispersed and detected in a CCD spectrometer. The spectral resolution of the spectrometer was estimated to be ∼3 nm, and because of the invariance of the optics and CCD over the wavelength range used, spectra were not corrected for instrument response. Excitation powers were on the order of ∼0.5−1 μW corresponding to intensities of ∼200−400 W/cm^2.

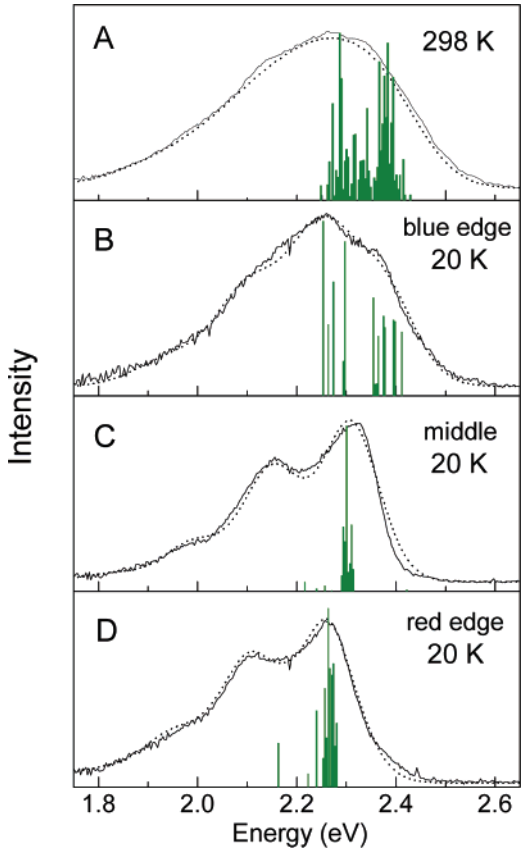

Figure 3. (A) Ensemble and fitted spectra of *long*-chain F8BT measured at 298 K. Stick spectra represent the amplitude (A) and E_0 of individual SM fits. Sorted subensemble and fitted spectra (20 K) of long-chain F8BT taken at different regions of the peak energy distribution in Figure 2C. (B) Blue edge (2.36−2.42 eV). (C) Middle (2.3−2.32 eV). (D) Red edge (2.17−2.27 eV).

Results and Discussion

In this study, large numbers of emission spectra of single isolated polymer chains of F8BT at ambient temperature (298 K) and low temperature (20 K) were acquired. Separate samples of short-chain F8BT and long-chain F8BT were studied. All spectra reported herein showed no evidence of flickering or other photoinduced processes during the time in which data were acquired (∼60 s). Typical individual SM spectra for F8BT samples at 20 K are shown in Figure 1. *Ensemble spectra* were constructed by simply summing the single polymer chain spectra, as shown, for example, in Figure 2B for long-chain F8BT at 298 K. The spectra were further analyzed by determining the emission energy of the spectral maxima, E_{max}, for each isolated chain. These values were used for two purposes. First, distributions of E_{max} were determined, e.g., Figure 2A, to obtain insights on the distributions of localized electronic transition energies within the ensemble. Second, the E_{max} values were used as the initial criterion for constructing subensemble spectra (e.g., Figure 3), which helped establish the main trends in the data. Interestingly, comparison of long- and short-chain E_{max} distributions from this work and previously reported room-temperature data[31] show virtually identical widths (∼0.2 eV), although both sets of samples had different polydispersities.

All observed spectra exhibit the expected vibronic pattern for a S_1-S_0 ($\pi^*-\pi$) emission transitions in polyfluorene copolymer systems with a dominant progression in a high-frequency CC stretching vibration (∼0.16 eV).[34] Cursory examination of the single-molecule (SM) spectra for long-chain F8BT reveal anecdotal evidence for the presence a bimodal distribution of spectral maxima, E_{max}. As shown in Figure 1, the set of spectra include examples of "blue" spectra, "red" spectra, and mixed (blue and red) spectra. The general trends are analogous to that previously observed for MEH-PPV.[2,15,35] The dual emission properties are emphasized by the vertical dotted lines in Figure 1. As described in the Introduction, low-energy "red" states in conjugated polymers arise from molecular packing effects (chain−chain contacts) that are believed to increase with increasing chain length, leading to lower transition energies.

The presence of a bimodal $G(E_{max})$ distribution for long-chain F8BT is especially apparent at 298 K, see Figure 2A. The appearance of distinct peaks for the "blue" and "red" forms for long-chain F8BT in Figure 2A at 298 K for the host polymer PMMA agrees with a previous observation of long-chain F8BT (M_n = 90 kDa) in a polystyrene host.[31] However, because of lower signal-to-noise ratios for long-chain spectra measured in ref 31, the bimodal behavior is not as distinct, as shown in Figure 2A. Surprisingly, a dual peak histogram is not actually observed at low temperature for long-chain F8BT, see Figure 2C. This appears to be due to an overlap of the "red" and "blue" peaks in the distribution. Evidence for this hypothesis is shown in parts B−D of Figure 3, which include *subensemble* long-chain F8BT spectra at 20 K for the blue, middle, and red portions of the ensemble, respectively. Qualitatively, the vibronic pattern of the blue subensemble is broader than the other subensembles and has a prominent blue shoulder, suggesting both blue- and red-emitting components. Comparison of the blue regions (ca. 2.3−2.4 eV) of peak energy histograms in Figure 2A and C show that the blue component shifts to lower energy at 20 K and coalesces with the red component, leading to the disappearance of the bimodal distribution. By sorting the 20 K long-chain spectra into subensembles, it is clear that there is not a continuous distribution of peak energies but, rather, overlapping discrete red and blue transitions. The different temperature dependence of bimodal components was also observed for low-temperature MEH-PPV SM spectra, which was attributed to an increase of effective conjugation lengths at low temperature.[33] This is discussed in more detail below, using an in-depth vibronic analysis, which incidentally was also used to determine the transition energies, E_0, employed in sorting the spectra for blue and red subensembles (Figure 3).

Interestingly the $G(E_{max})$ distribution for short-chain F8BT shows very little evidence for the red-emitting form at 298 or 20 K, see Figure 4. Short-chain SM spectra also show broad and unresolved line shapes with lower signal-to-noise ratios than long-chain samples and do not change between 298 and 20 K (data not shown). Apparently, the small chain length prohibits the formation of chain−chain contacts, decreasing the number of red-emitting sites per polymer chain. This result is consistent with the previous observation that short-chain F6BT (M_n = 9 kDa) also lacked a bimodal distribution and emits exclusively from blue sites.[31] It is also consistent with studies on MEH-PPV that have shown that shorter chains contain a considerably smaller number of red sites.[15] The spectroscopic consequence of chain−chain contacts is even apparent in the 20 K ensemble spectra of F8BT, which are summarized in Figure 5. A comparison of short- (Figure 5A) and long-chain (Figure 5B) single-molecule ensemble spectra at 20 K reveal that the latter is significantly shifted to lower emission energies due to red sites. As in the case of MEH-PPV, only a small number, even one, intrachain contact is sufficient to funnel the energy to low-energy-emitting chromophores. Figure 5C portrays an ensemble

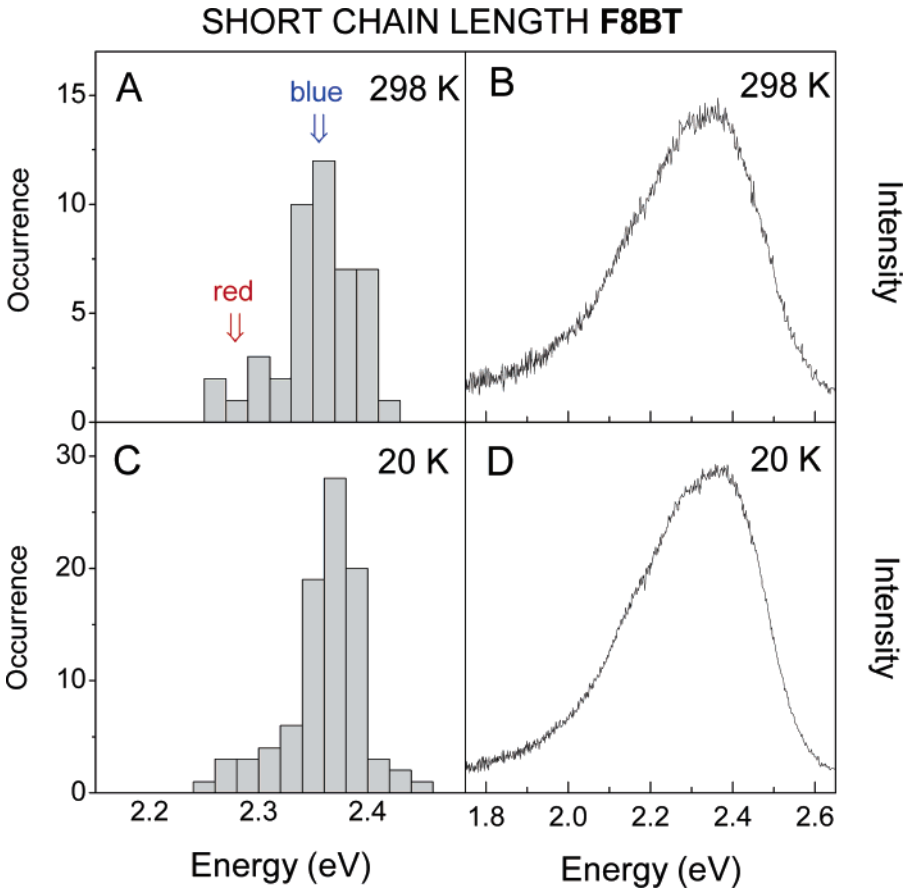

Figure 4. Emission peak energy distributions and ensemble emission spectra for isolated *short* chains of F8BT dissolved in a PMMA thin film at 298 K (A, B) and 20 K (C, D).

spectrum of a bulk F8BT film measured at 20 K (which is identical for *either* short or long polymer chains). This suggests that, in the bulk polymer, interchain contacts are sufficient to efficiently funnel the energy to red sites, and intrachain contacts are not necessary for the red site effect.

To gain further insight into the spectral line shape of F8BT, we performed a vibronic analysis on each of the single-chain spectra measured at 298 and 20 K. Typically, SM spectra were fit with either one or two chromophores by using an effective mode model to obtain an acceptable fit. The vibronic intensity distributions of each chromophore were fit to the following expression,

$$I_{\mathrm{em}} = A\omega^3 \sum_{n_i=0} \frac{e^{-S_i} S^{n_i}}{n_i!} e^{-[(\omega - E_0 + n_i \hbar\omega_i)/\sigma]^2} \qquad (1)$$

where A is a constant, ω is the frequency of emitted light, and S is the Huang−Rhys factor in dimensionless units. In this model, the vibronic transitions are broadened by a Gaussian function, with E_0 representing the energy of the electronic origin (0−0) for each chromophore, n_i is number of vibrational quanta, and σ is the line width (fwhm). Spectra were fitted with one high-frequency mode (0.16 eV), corresponding to a CC stretching vibration.[34] The necessary S and σ parameters were adjusted to achieve a good fit with experiment. Because Franck−Condon active low-frequency modes, such as torsional vibrations (<100 cm^{-1}) localized on the chain backbone,[36−39] cannot be resolved with our instrument, these degrees of freedom are taken into account here by the Gaussian spectral-broadening term. For *long-chain* spectra showing evidence for multichromophore transitions, i.e., nonreplica vibronic patterns and overlapping shoulders, the highest energy resolved features in the spectrum are chosen as the E_0 of each chromophore. We use only one chromophore to fit *short-chain* F8BT SM spectra due to the lack of resolved vibronic structure and temperature invariant emission line shapes.

Figure 1 compares fitted spectra to the experimental spectra for representative individual polymer chains. Subensemble (Figure 3) and ensemble (Figure 5) fitted spectra of long-chain F8BT were obtained by simply summing the individual fitted spectra from the molecules in the appropriate set. Stick spectra representing the amplitude (A) and E_0 of each chromophore used in fitting all SM spectra show a similar bimodal behavior to the $G(E_{\mathrm{max}})$ for long-chain F8BT spectra measured at 298 K (see Figure 3A), confirming the bimodal character of the distribution. The distribution of E_0 values at 20 K is also much narrower than at 298 K, and at 20 K, the bimodal character is masked due to overlapping blue and red transitions. Sorted "blue edge" subensemble spectra (Figure 3B) demonstrate that the distinctly different vibronic patterns are due to overlapping blue and red transitions, while spectra chosen near the maximum (Figure 3C) and the red edge (Figure 3D) of the peak energy histogram have similar line shapes corresponding to transitions from only red chromophores. Stick spectra and line shapes of the 20 K "blue-edge" subensemble with the 298 K total ensemble (Figure 3A) also show excellent agreement, which further confirms the presence of two distinct emitting species.

The spectral line shapes of long-chain F8BT show considerable variation between molecules measured at the same temperature. This is reflected in the distributions of the Huang−Rhys factors, S (Table 1), which is probably the result of variations in conformations or interactions between the mol-

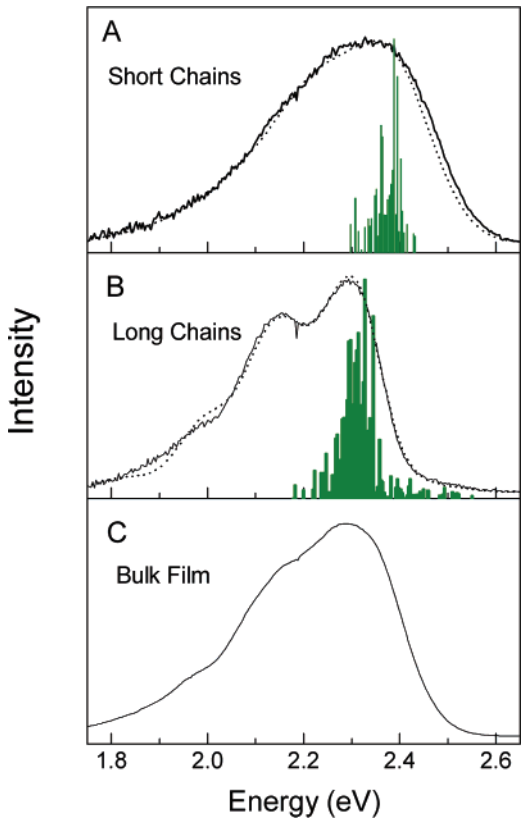

Figure 5. Experimental (solid lines) and fitted (dashed lines) ensemble spectra for *short*-chain (A) and *long*-chain F8BT (B) measured at 20 K. Ensemble fitted spectra were generated from summing single-molecule spectra fits. "Stick" spectra represent the amplitude and E_0 for each chromophore used in the simulations. (C) Bulk film spectrum measured at 20 K.

TABLE 1: Average Best-Fit Parameters for *Short*- and *Long*-Chain F8BT Ensemble and Subensemble Spectra Measured at 20 and 298 K[a]

	short chains[b]	long chains		
	20 K	20 K	298 K blue	298 K red
$\langle S \rangle$ (dimensionless)	0.48 ± 0.023	0.49 ± 0.084	0.61 ± 0.080	0.55 ± 0.038
$\langle \sigma \rangle$ (eV)	0.11	0.087	0.11	0.12
$\langle E_0 \rangle$ (eV)	2.38 ± 0.028	2.32 ± 0.061	2.38 ± 0.019	2.30 ± 0.018

[a] Vibrational frequencies used for calculated spectra were 0.16 eV for both *short* and *long* chains. [b] There were no significant changes in average parameter values for short-chain samples between 298 and 20 K.

ecules and the host matrix. As shown in Table 1, long-chain samples also show a small but significant decrease in the S parameter values at low temperature. In addition, there is a decrease of σ with decreasing temperature, reflecting the usual sharpening of a spectrum due to a decreased intensity of hot bands as the temperature is lowered. The decrease of both S and σ at low temperature indicates a temperature-induced structural change, possibly due to a cooling of displaced torsional modes. These low-frequency vibrations are known to lead to disorder along the chain,[38,40] causing a decrease in conjugation lengths. Freezing out these degrees of freedom could lead to an increase of effective conjugation lengths and, consequently, a red-shift of emission energies and collapse of the bimodal distribution at low temperature.

Conclusions

Single-molecule spectroscopy of long-chain F8BT has revealed that emission peak energy distributions, $G(E_{max})$, are bimodal in character. Intramolecular chain−chain contacts, which are more common in long-chain samples, are responsible for efficient energy migration to low-energy sites, which leads to the "red" emitting form. Short-chain F8BT molecules simply lack this feature and only emit from higher-energy "blue" chromophores. The collapse of the bimodal distribution at ~20 K for long-chain F8BT may result from an increase in effective conjugation lengths due to freezing out of low-frequency torsional vibrations. This is supported by the decrease of S and σ values from the vibronic analysis of SM line shapes.

Acknowledgment. We gratefully acknowledge support of the National Science Foundation and the Welch Foundation for support of this research. J.K.G. acknowledges the Petroleum Research Fund of the American Chemical Society for a fellowship, and J.S.K. thanks the EPSRC for an Advanced Research Fellowship.

References and Notes

(1) Hu, D.; Yu, J.; Barbara, P. F. *J. Am. Chem. Soc.* **1999**, *121*, 6936.
(2) Yu, J.; Hu, D.; Barbara, P. F. *Science* **2000**, *289*, 1327.
(3) Hu, D.; Yu, J.; Wong, K.; Bagchi, B.; Rossky, P. J.; Barbara, P. F. *Nature* **2000**, *405*, 1030.
(4) Peng, K. Y.; Chen, S. A.; Fann, W. S. *J. Am. Chem. Soc.* **2001**, *123*, 11388.
(5) Schwartz, B. J. *Annu. Rev. Phys. Chem.* **2003**, *54*, 141.
(6) Peng, K. Y.; Chen, S. A.; Fann, W. S.; Chen, S. H.; Su, A. C. *J. Phys. Chem. B* **2005**, *109*, 9368.
(7) Ariu, M.; Lidzey, D. G.; Bradley, D. D. C. *Synth. Met.* **2000**, *111−112*, 607.
(8) Scherf, U.; List, E. J. W. *Adv. Mater.* **2002**, *14*, 477.
(9) Khan, A. L. T.; Sreearunothai, P.; Herz, L.; Banach, M. J.; Köhler, A. *Phys. Rev. B* **2004**, *69*, 085201.
(10) Chunwaschirasiri, W.; Tanto, B.; Huber, D. L.; Winokur, M. J. *Phys. Rev. Lett.* **2005**, *94*, 107402: 1.
(11) Becker, K.; Lupton, J. M. *J. Am. Chem. Soc.* **2005**, *127*, 7306.
(12) VandenBout, D. A.; Yip, W. T.; Hu, D. H.; Fu, D. K.; Swager, T. M.; Barbara, P. F. *Science* **1997**, *277*, 1074.
(13) Wang, C. F.; White, J. D.; Lim, T. L.; Hsu, J.-H.; Yang, S.-C.; Fann, W.-S.; Peng, K.-Y.; Chen, S.-A. *Phys. Rev. B* **2003**, *67*, 035202.
(14) Schindler, F.; Lupton, J. M.; Feldmann, J.; Scherf, U. *Proc. Natl. Acad. Sci. U.S.A.* **2004**, *101*, 14695.
(15) Kim, D. Y.; Grey, J. K.; Barbara, P. F. *Synth. Met.* **2006**, *156*, 336.
(16) Pullerits, T.; Mirzov, O.; Scheblykin, I. *J. Phys. Chem. B* **2005**, *109*, 19099.
(17) Huser, T.; Yan, M.; Rothberg, L. J. *Proc. Natl. Acad. Sci. U.S.A.* **2000**, *97*, 11187.
(18) Gronheid, R.; Hofkens, J.; Köhn, F.; Weil, T.; Reuther, E.; Müllen, K.; De Schryver, F. *J. Am. Chem. Soc.* **2002**, *124*, 2418.
(19) Cotlet, M.; Gronheid, R.; Habuchi, S.; Stefan, A.; Barbafina, A.; Müllen, K.; Hofkens, J.; De Schryver, F. *J. Am. Chem. Soc.* **2003**, *125*, 13609.
(20) Cotlet, M.; Vosch, T.; Masuo, S.; Sauer, M.; Muellen, K.; Hofkens, J.; De Schryver, F. *Prog. Biomed. Opt. Imaging, SPIE* **2004**, *5322*, 20.
(21) Cotlet, M.; Vosch, T.; Habuchi, S.; Weil, T.; Muellen, K.; Hofkens, J.; De Schryver, F. *J. Am. Chem. Soc.* **2005**, *127*, 9760.
(22) Angeles Izquierdo, M.; Bell, T. D. M.; Habuchi, S.; Fron, E.; Pilot, R.; Vosch, T.; De Feyter, S.; Verhoeven, J.; Hofkens, J.; De Schryver, F.; Jacob, J.; Muellen, K. *Chem. Phys. Lett.* **2005**, *401*, 503.
(23) Gesquiere, A. J.; Uwada, T.; Asahi, T.; Masuhara, H.; Barbara, P. F. *Nano Lett.* **2005**, *5*, 1321.
(24) Morteani, A. C.; Dhoot, A. S.; Kim, J.-S.; Silva, C.; Greenham, N. C.; Murphy, C.; Moons, E.; Ciná, S.; Burroughes, J.; Friend, R. H. *Adv. Mater.* **2003**, *15*, 1708.
(25) Kim, J.-S.; Ho, P. K. H.; Murphy, C. E.; Friend, R. H. *Macromolecules* **2004**, *37*, 2861.
(26) Stevens, M. A.; Silva, C.; Russell, D. M.; Friend, R. H. *Phys. Rev. B* **2001**, *63*, 165213.
(27) Snaith, H. J.; Arias, A. C.; Morteani, A. C.; Silva, C.; Friend, R. H. *Nano Lett.* **2002**, *2*, 1353.
(28) Kietzke, T.; Neher, D.; Kumke, M.; Montenegro, R.; Landfester, K.; Scherf, U. *Macromolecules* **2004**, *37*, 4882.
(29) Kim, Y.; Cook, S.; Choulis, S. A.; Nelson, J.; Durrant, J. R.; Bradley, D. D. C. *Chem. Mater.* **2004**, *16*, 4812.
(30) Watkins, P. K.; Walker, A. B.; Verschoor, G. L. B. *Nano Lett.* **2005**, *5*, 1814.

(31) Lammi, R. K.; Barbara, P. F. *Photochem. Photobiol. Sci.* **2005**, *4*, 95.
(32) Bernius, M. T.; Inbasekaran, M.; O'Brien, J.; Wu, W. *Adv. Mater.* **2000**, *12*, 1737.
(33) Yu, Z.; Barbara, P. F. *J. Phys. Chem. B* **2004**, *108*, 11321.
(34) Donley, C. L.; Zaumseil, J.; Andreasen, J. W.; Nielsen, M. M.; Sirringhaus, H.; Friend, R. H.; Kim, J.-S. *J. Am. Chem. Soc.* **2005**, *127*, 12890.
(35) Rønne, C.; Trägårdh, J.; Hessman, D.; Sundström, V. *Chem. Phys. Lett.* **2004**, *388*, 40.
(36) Karabunarliev, S.; Baumgarten, M.; Bittner, E. R.; Muellen, K. *J. Chem. Phys.* **2000**, *113*, 11372.
(37) Karabunarliev, S.; Bittner, E. R.; Baumgarten, M. *J. Chem. Phys.* **2001**, *114*, 5863.
(38) Tretiak, S.; Saxena, A.; Martin, R. L.; Bishop, A. R. *Phys. Rev. Lett.* **2002**, *89*, 097402.
(39) Bittner, E. R.; Karabunarliev, S. *J. Chem. Phys.* **2003**, *118*, 4291.
(40) Franco, I.; Tretiak, S. *J. Am. Chem. Soc.* **2004**, *126*, 12130.